Use of laser-diode arrays in holographic interconnections

Betty Lise Anderson, Thomas B. De Vore, and Bradley D. Clymer

Holographic interconnection schemes for high-speed data transfer have been demonstrated by other researchers. Because holographic recording materials presently available are sensitive to the visible spectrum but not to the near infrared, these studies used bulky gas lasers. Visible laser diodes, as they become available, will likely become a preferred source in a practical system because of their small size and high beam powers. The two mutually coherent beams needed to write the hologram have previously been implemented by using bulk optics to split a beam. In anticipation of the use of coherently coupled visible laser diode arrays as sources, it is shown that the individual elements of laser diode arrays currently available have sufficient mutual coherence to create reasonable holographic elements. This application is demonstrated with an infrared array because of the unavailability of visible arrays in this emerging technology. It is extrapolated that for visible coherently coupled laser diode arrays and current holographic materials, a holographic interconnection system is potentially feasible by using the mutually coherent beams from individual facets. This makes recording holograms more straightforward because the recording process eliminates beam splitting requirements. Therefore the system is more desirable for *in situ* recording situations such as those required for dynamic interconnection.

Key words: Holographic interconnections, diode arrays, coherence, visible laser diodes.

Introduction

The ability to perform global interconnection for several data paths with holograms and bulk optical elements has been well established in the literature.[1] Holograms can be used to route an optical stream of data to a specific destination. In a static system a fixed hologram (for example, made on film) directs data from source A to detector B. In a dynamic system the hologram is recorded such that the data beam is directed from source A to detector B for a time, and then the hologram is reprogrammed to direct the data to detector C for the next interval.

An example of a holographic interconnection system is shown in Fig. 1. In Fig. 1(a) a Fourier hologram is formed by interfering two plane waves. The plane waves are generated by using the optical Fourier-transform geometry shown. The light emitters at x_1 and x_2 are placed in the front focal plane of the lens, and the hologram is placed at the other focal plane. The wave vectors of the beams are $\mathbf{k}_1$ and $\mathbf{k}_2$, respectively. The waves interfere to form fringes perpendicular to $\mathbf{k}_h$, which is the vector difference of $\mathbf{k}_1$ and $\mathbf{k}_2$.

Upon reconstruction, a single source is activated. Light from this source is directed to a focused spot at the detector, as shown in Fig. 1(b). During reconstruction, the plane wave from the first Fourier-transform lens is incident at the Bragg angle of the hologram grating, diffracting light at the output Bragg angle as if propagating from the other source. The second Fourier-transform lens focuses this beam to a spot at the image of the other source. For example, if the source at x_1 is activated, light is diffracted and focused to $-x_2$ at the receiver plane on the right. Conversely, if x_2 is activated, light is diffracted and focused to $-x_1$ in the receiver plane. Both x_1 and x_2 sources can be activated simultaneously, with cross talk at the receiver plane being a function of the diffraction efficiency of the hologram.

For dynamic interconnection the hologram can be recorded by using a high-power strobe in which both sources are on. Data transfer can then occur with low-power modulation of one or both of the sources until the hologram is erased by illumination.

The sources in the emitter plane must be mutually

When this work was performed, all the authors were with Dreese Laboratory, Department of Electrical Engineering, The Ohio State University, 2015 Neil Avenue, Columbus, Ohio 43210. T. B. De Vore is now with International Business Machines Corporation, 1001 W. T. Harris Boulevard, Building 251, Department 21N, Charlotte, N.C. 28257.

Received 5 March 1992.
0003-6935/92/357411-06$05.00/0.

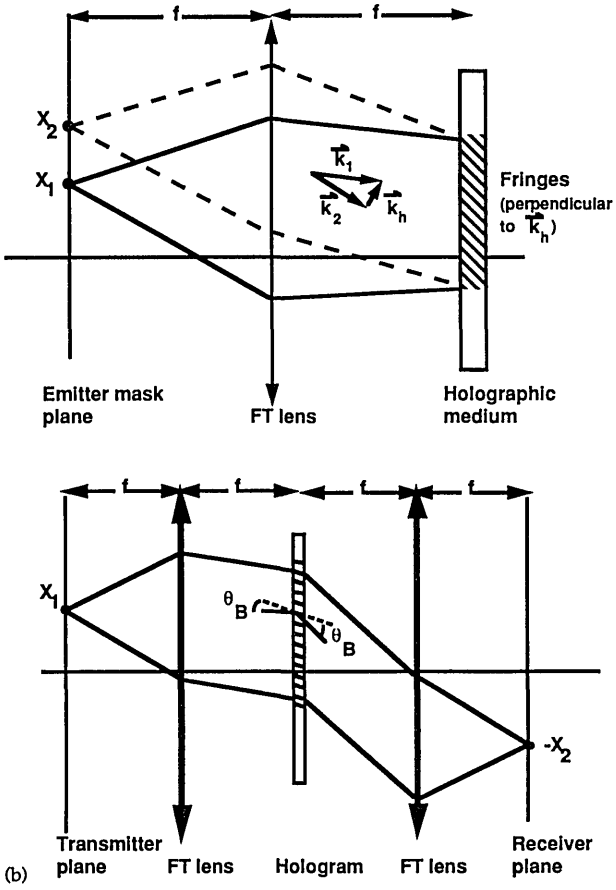

Fig. 1. (a) Recording geometry for interconnection hologram. (b) Reconstruction geometry for interconnection. FT lenses, Fourier-transform lenses; θ_B, Bragg angles.

coherent to record the hologram. Control of the positions of the sources used for recording the hologram is key to controlling the interconnection pattern. The ability to switch the output beams of a laser diode array therefore permits various interconnection patterns to be recorded.

For example, to electronically select specific emitters in the laser diode array, we could implement external modulators as shown in Fig. 2. In order to maintain coherence between all the emitters, all of the stripes must be lasing simultaneously. To block the emissions from all but the selected sources, we would need the modulators to be individually addressable. Recent research in devices exploiting the quantum-confined Stark effect[2–4] as well as electrorefraction[5] shows that high bandwidths (up to 40 MHz) and high-contrast modulation (20 dB or more) are achievable. Research on these modulators has, however, concentrated on infrared devices to date. Alternatively, the Kerr effect might be used to rotate the polarizations of the unwanted beams so that they cannot interfere with the selected beams. (Laser diode beams generally have a high polarization purity.)

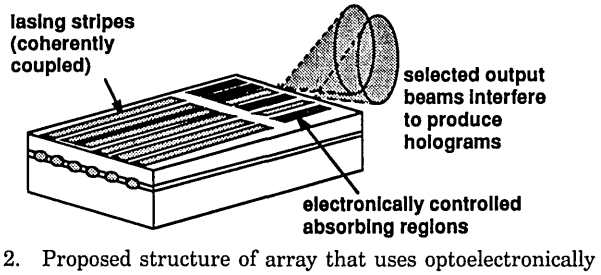

Fig. 2. Proposed structure of array that uses optoelectronically integrated external modulators to select emitters.

Visible light is traditionally used for both static and dynamic holography because of the responsivity and the spatial resolution of the materials available for recording the fringes. Visible laser-diode arrays are currently not commercially available, but research devices have been reported.[6,7] In order to show the feasibility of our approach, we performed experiments with infrared arrays, and we assumed that similar coherence and output powers are likely with visible sources.

Experiment

Two mutually coherent beams interfere together to produce a hologram. The fringes are recorded in an intensity- or phase-recording medium, and when one of the beams is projected upon the hologram, its intensity or phase is modulated. To avoid splitting a single beam (and thus avoid bulk optics), we propose using the various elements of a laser diode array as sources and reference beams. Consider a coherently coupled laser array with ten elements. When the array is on, each element is lasing, but because of their physical proximity to one another, their evanescent fields overlap and they are coherently coupled. Each element therefore has some degree of coherence with each of the others. In general, elements that are adjacent or physically close were found to have higher mutual coherence than those farther apart.

A Spectra Diode Labs SDL2410 coherently coupled laser diode array was used in the experiments described here. The device has a nominal wavelength of 820 nm and a maximum output power of 100 mW cw. It has ten emitters, separated by 10 μm center-to-center. Thus the emitting area is approximately 100 μm × 1 μm.

Mutual Coherence

The mutual coherence was measured by blocking the emission from all but the selected emitters and by measuring the visibility of the fringe pattern. The emissions here were selected by using slits (produced on photographic film). The small size of the emitters, with beam waists that the manufacturer specifies to be approximately 2.5 μm, made it necessary to magnify the near field to a more tractable size. The near field was magnified by a factor of 6.45, which increased the beam waists to 16.1 μm and the spacing between emitters to 64.5 μm.

By passing the radiation from only selected emitters, we essentially employ Young's method. Note that the fringes in the hologram are caused by a path-length difference, which in turn causes the necessary phase difference. It is therefore essential that the sources have sufficient temporal coherence such that the fringe pattern is not mitigated by excessive path length. Examination of the spectrum of the array showed that it oscillated in two or three longitudinal modes; we calculated a worst-case temporal coherence length of 1.227 mm at $1.2I_{th}$. The threshold current was 203 mA. The coherence length is much greater than the emitter spacing, so it exceeds the greatest possible path-length difference (by a factor of nearly 20). We therefore neglect temporal coherence effects from here on.

Figure 3 shows the intensity distribution of a cross section of the magnified near-field image. The distribution was recorded by scanning an optical fiber (core diameter of 5 μm) across the image plane. The emitters are numbered from left to right. Note that emitters 5 and 6 each exhibit a double lobe, indicating that these laser stripes are not oscillating in the fundamental transverse mode.

To measure the mutual coherence between two emitters, we blocked the other emitters (in the magnified near-field plane) and recorded the resulting interference pattern. As before, the intensity distribution (this time of the fringe pattern) was obtained by scanning an optical fiber across the pattern. A motorized translating stage and a data acquisition board were used with a personal computer to obtain the data.

The magnitude of the mutual coherence between sources A and B is obtained by

$$\gamma_{AB}(\tau) = \frac{V}{R}, \tag{1}$$

where R and V depend on the intensities I of each

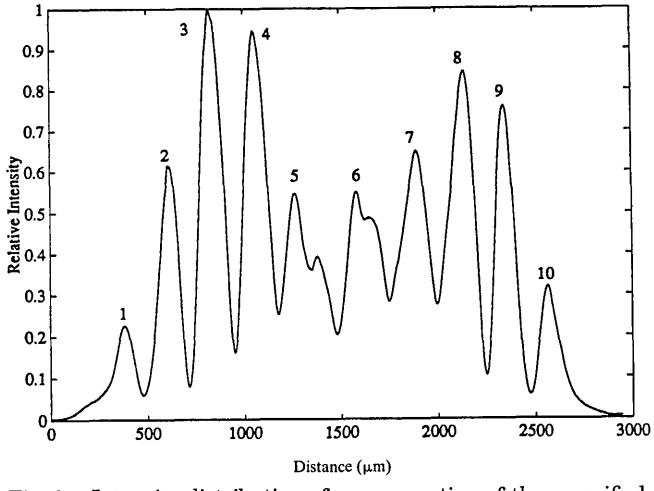

Fig. 3. Intensity distribution of a cross section of the magnified near field of the laser array. The emitters are numbered from left to right. The image is magnified by a factor of 6.45.

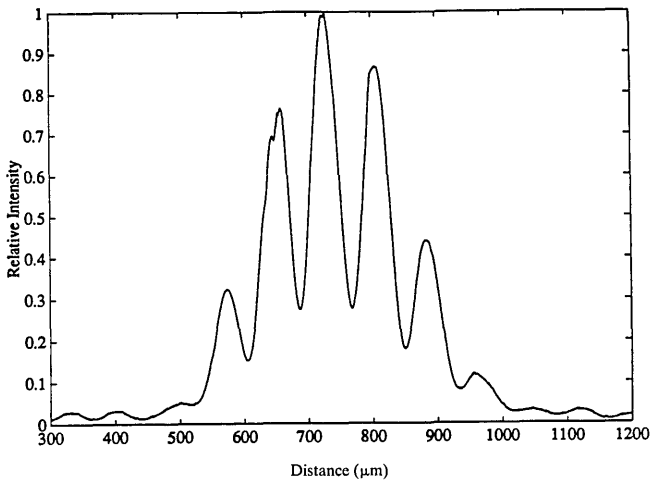

Fig. 4. Intensity distribution of the fringe pattern from interference between emitters 8 and 9 (mutual coherence is 0.868).

source:

$$V = \frac{I_{max} - I_{min}}{I_{max} + I_{min}},$$

$$R = \frac{2\sqrt{I_A}\,\sqrt{I_B}}{I_A + I_B}. \tag{2}$$

The relative intensities to calculate R were taken from Fig. 3. A typical interference pattern intensity distribution, in this case between emitters 8 and 9, is shown in Fig. 4. From this figure the visibility is measured.

Table 1 summarizes the mutual coherence data for the six emitter pairs measured. The maximum coherence is 0.868, which is for adjacent emitters 8 and 9. The minimum was 0.096 for emitters 1 and 10, which, while still measurable, is extremely low.

We did not measure mutual coherence as a function of current for our array because at many currents it oscillated in a large number of longitudinal modes, which reduced the temporal coherence and therefore compromised the validity of the results. Previous research has shown, however,[8] that the spatial coherence of the beam (as measured in the far field) from this type of array is not a strong function of drive

Table 1. Relative Intensity, Visibility, and Coherence Data for Various Emitter Pairs in SDL 2410 Laser Diode Array[a]

Emitter Pair	Relative Intensity Value	Visibility	Mutual Coherence
3, 4	0.999	0.802	0.802
3, 5	0.954	0.536	0.562
5, 6	1.000	0.595	0.595
8, 9	0.997	0.865	0.868
4, 7	0.973	0.120	0.123
1, 10	0.951	0.092	0.096

[a] $\lambda = 820$ nm.

current. In Ref. 8 the authors measured not the mutual coherence between selected emitters but rather the spatial coherence of the total beam resulting from the emissions from all stripes. The spatial coherence was zero below lasing threshold, increased rapidly just above threshold, and saturated at $1.01I_{th}$. The magnitude of the spatial coherence was between 0.8 and 1.0 near the beam center. (Similar experiments for single-stripe lasers resulted in spatial coherence saturation at $\sim 1.2I_{th}$, where $|\gamma| = 1.0$.) Note that this behavior is different from that of temporal coherence, which generally increases monotonically with optical power. The spatial coherence is not improved by operating the laser at a higher current level, although the total optical power, and therefore the error rate, is improved.

Implications for Holography

The medium used for recording holograms must be sensitive to the wavelengths of the source. It should also have high resolution so that a large number of fringes can be recorded per unit area, increasing the efficiency.

We attempted to create holograms on photographic film by using two selected emitters from the laser array. The array wavelength is 820 nm, so we selected Kodak 4143 ESTAR thick-base high-speed infrared film. This film has a maximum sensitivity in the 750–840-nm region, but its resolving power is 80 lines/mm or 40 line pairs/mm. This is poor compared with visible-range films (resolving power ~5000 line pairs/mm). Figure 5 is a photograph, taken through a microscope, of the fringe pattern produced by interfering the beams from adjacent emitters 3 and 4. The fringe spacing is ~50 μm. The photograph is too grainy to even measure the fringe visibility, which should ideally be equal to the mutual coherence between these emitters (since they have equal intensities), or 0.802. The visibility of the fringes recorded is always slightly less than the visibility of the actual interference pattern, however, owing to scattering in the medium.[9]

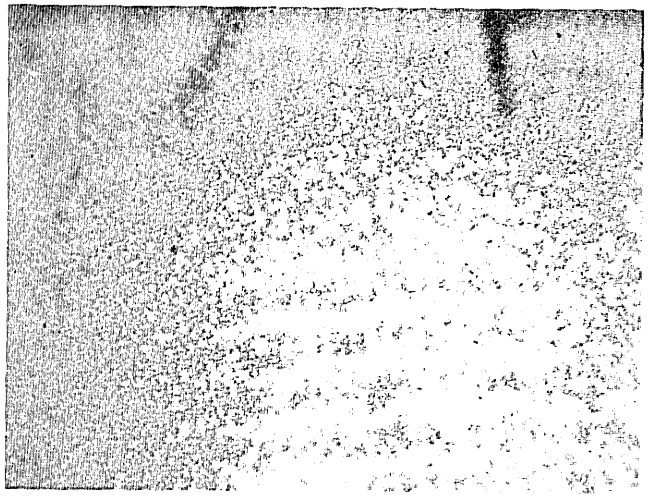

Fig. 5. Fringe pattern recorded on Kodak 4143 ESTAR thick-base high-speed infrared film; the pattern is produced by using emitters 3 and 4 (mutual coherence is 0.802). The wavelength is 820 nm.

To investigate the efficiency of holograms produced by using a diode array, we assumed that a future laser diode array emitting at visible wavelengths would have coherence properties comparable with those of the 820-nm array that we measured. We use these values of mutual coherence (actually visibility, as explained below) between the sources to predict efficiency for known holographic recording media.

The diffraction efficiency, defined as the power diffracted by a hologram divided by the power incident upon the hologram, is obtained by[9]

$$\epsilon = \tfrac{1}{4}[\beta\langle E\rangle V(s)M(s)]^2, \tag{3}$$

where $\langle E\rangle$ is the average exposure, s is the spatial frequency of the fringes, $V(s)$ is the visibility of the interference fringes formed, and $M(s)$ is the modulation transfer function of the recording medium. The quantity β represents the slope dt/dE of the amplitude transmittance t evaluated at $\langle E\rangle$. Assuming β and $M(s)$ to be fixed, we see that the diffraction efficiency depends on the square of the visibility of the interference fringes. Table 2 gives some values from Ref. 9 of maximum diffraction efficiencies for various recording media. These maxima assume perfect mutual coherence, or visibility of 1.0. By using our measured values of visibility (for the infrared diode array) in Eq. (3) and values of $[\beta M(s)]^2$ calculated from the table, we calculate the hologram diffraction efficiencies for the best-case visibility that we observed in this particular array (0.86 for emitters 8 and 9). Finally, it should be noted that the experimental visible laser diode arrays reported in the literature[6,7] emit at 660 nm, which is outside the sensitive range of some of the media. This is particularly important for dynamic interconnections, which rely on photorefractive crystals sensitive in the 350–550-nm range. Arrays emitting in the 500-nm range are presumably not in our near future.

Table 2. Various Holographic Recording Media and Their Maximum Diffraction Efficiencies Assuming a Source Emitting in the Sensitive Wavelength Range[a]

Recording Medium	Wavelength Range (nm)[b]	Max ϵ for V = 1.0[b]	Max ϵ for V = 0.868
Photographic emulsion (bleached)	400–700	0.6	0.45
Dichromated gelatin	350–580	0.9	0.67
Photoresists	UV–500	0.3	0.22
Photopolymers	UV–650	0.9	0.67
Photothermoplastics	400–650	0.3	0.22
$LiNbO_3$	350–500	0.2	0.15
$Bi_{12}SiO_{20}$	350–550	0.25	0.19

[a]The final column shows the maximum efficiency one could expect given a laser diode array having the same visibility as the maximum we measured and given that the emitting wavelength is in the sensitive region.

[b]See Ref. 9.

Discussion

Because the diffraction efficiency of a hologram depends on the visibility of the fringes produced by the two interfering beams, we measured the visibility and mutual-coherence values for various pairs of emitters on a Spectra Diode Labs SDL2410 coherently coupled laser diode array emitting at 820 nm. The maximum mutual coherence observed was $\gamma = 0.868$ for two adjacent emitters (visibility $V = 0.865$). Emitters separated by one emitter had a maximum $\gamma = 0.562$ ($V = 0.536$). The two end emitters (eight emitters in between) have virtually no mutual coherence, with $\gamma = 0.096$ ($V = 0.092$).

The diffraction efficiency of a hologram increases as the square of the visibility of the sources, so the efficiency drops off considerably as emitters are spaced farther apart. Choosing photographic film as an arbitrary example, we see that a source with perfect visibility results in $\epsilon = 0.6$, meaning that 60% of the energy hitting the hologram is diffracted to the correct destination. Adjacent emitters 8 and 9 produce a visibility of 0.802, resulting in an ϵ of 0.45. Emitters separated by one stripe (emitters 3 and 5) give a visibility of the order of 0.53, resulting in $\epsilon = 0.17$, already not usable. This last number is only slightly mitigated by the fact that the intensities of emitters 3 and 5 are different (see Fig. 3), which reduces the visibility. Their mutual coherence is 0.562, causing $\epsilon = 0.19$.

It should be noted that present-day diode arrays are designed for high-power applications, and they tend to optimize far-field intensity distribution and beam divergence rather than high coherence. Scifres *et al.* have shown that there is an optimum spacing for good output patterns.[10] Closer stripe spacing, however, should increase interstripe field coupling and therefore improve coherence. It is therefore possible that present-day devices could be optimized toward coherence improvement, since the total output beam pattern would not be used as such in the application described here. It is reasonable to expect that, when the interstripe spacing becomes too small, the array would begin to behave as a broad-area laser, resulting in filamenting, spurious interference patterns, and unpredictable field patterns. This puts a lower limit on the interemitter spacing, and further research is needed to assess the limits on interemitter coherence.

Summary

Although holographic optical interconnections are expected to greatly increase data transfer rates, recording media currently available are generally sensitive to visible wavelengths. This, combined with the necessity for two mutually coherent beams, has called for the use of high-power lasers such as gas lasers. These are physically too large for a practical system. Additional bulk is added by the beam splitters and other bulk optics to produce the two beams needed to make the hologram. A laser diode array has a small physical size, and the emitters are coherently coupled, so that two of the emitters could be used to produce and read holograms. Currently available arrays emit only in the infrared, but visible arrays, with wavelengths that are compatible with existing holographic materials, are anticipated soon.

We have therefore examined the possibility of using laser diode arrays in future optical interconnection systems. By selecting individual beams from the array, the hologram can be written and read, as long as the two beams are sufficiently mutually coherent. Present-day holographic materials (film, gelatins, and $LiNbO_3$, to name a few) are sensitive to wavelengths in the UV to visible range, whereas present-day laser diode arrays emit only in the near infrared (~ 800 nm and higher). Dynamic interconnections require electrorefractive materials, which are sensitive to wavelengths of 550 nm and lower. At the present time, therefore, use of the arrays for holographic interconnections is not feasible. We chose, however, to use a present-day commercially available infrared diode array to extrapolate to future visible-emitting arrays, which are currently under development.

Assuming that holographic recording materials remain much as they are today, but also assuming that laser diode arrays of the future emit in the visible range, we project diffraction efficiencies approximately 75% of what is currently obtainable with perfectly mutually coherent sources, such as a power-split gas laser beam. This result is for two adjacent emitters in the array; for emitters separated by one emitter, this decreases to 25%.

Nevertheless, we believe there is some room for improvement in the mutual coherence between emitters of the array; current devices are intended for high-power applications, and as such, they are not optimized toward coherence but rather toward beam output pattern. Furthermore, we anticipate the possibility of using electroabsorptive follower regions in the arrays to electronically turn on and off selected emitters while preserving the overall mutual coherence.

The use of laser diode arrays will greatly improve the physical size, the operating efficiency, and the cost of holographic interconnection systems such as those described in the Introduction. The elimination of bulk optics will also reduce fabrication difficulties. In this study, the individual elements were selected by using a mask, which is not a practical system in real life. The possibility of on-chip optical modulators would eliminate the need for physical slits, again reducing fabrication costs and size and increasing speed of operation.

References

1. J. W. Goodman, F. J. Leonberger, S.-Y. Kung, and R. A. Athale, "Optical interconnections for VLSI systems," Proc. IEEE **72,** 850–866 (1984).
2. J. E. Zucker, I. Bar-Joseph, B. I. Miller, U. Koren, and D. S. Chemla, "Quaternary quantum wells for electro-optic intensity and phase modulation at 1.3 and 1.55 μm," Appl. Phys. Lett. **54,** 10–12 (1988).
3. S. Nojima and K. Wakita, "Optimization of quantum well

materials and structures for excitonic electroabsorption effects," Appl. Phys. Lett. **53,** 1958–1960 (1988).
4. K. Wakita, I. Kotaka, H. Asai, M. Okamoto, Y. Kondo, and M. Nagauma, "High-speed and low-drive-voltage monolithic multiple quantum well modulator/DFB laser light source," IEEE Photon. Technol. Lett. **4,** 16–18 (1992).
5. S. Nojima, "Enhancement of excitonic electrorefraction by optimizing quantum well materials and structures," Appl. Phys. Lett. **55,** 1868–1870 (1989).
6. A. Valster, J. P. Andre, E. Dupont-Nivet, and G. M. Martin, "High-power AlGaInP three-ridge type laser diode array," Electron. Lett. **24,** 326–327 (1988).
7. A. Valster, J. Opschoor, R. Drenten, C. v. d. Poel, and J. P. Andre, "Phase-locked Y-coupled index-guided visible light (660 nm) semiconductor laser array," in *Proceedings of 11th IEEE International Semiconductor Laser Conference* (Institute of Electrical and Electronics Engineers, New York, 1988), p. 231.
8. B. L. Anderson and P. L. Fuhr, "Measurement of spatial coherence of quantum-well laser diodes," in *Annual Meeting,* Vol. 18 of 1989 OSA Technical Digest Series (Optical Society of America, Washington, D.C., 1989), paper ThR5.
9. P. Hariharan, *Optical Interferometry* (Academic, Orlando, Fla., 1985).
10. D. R. Scifres, W. Streifer, and R. D. Burnham, "Experimental and analytic studies of coupled multiple stripe diode lasers," IEEE J. Quantum Electron. **QE-15,** 917–922 (1979).